



Oxidative stability of microalgae oil and its acylglycerol mixture obtained by enzymatic glycerolysis and the antioxidant effect of supercritical rosemary extract

Celia Bañares^a, Assamae Chabni^a, Guillermo Reglero^{a,b}, Carlos F. Torres^{a,*}

^a Department of Production and Characterization of Novel Foods, Institute of Food Science Research (CIAL, CSIC-UAM), C/ Nicolas Cabrera 9, 28049, Madrid, Spain

^b Department of Production and Development of Foods for Health, IMDEA-Food Institute, CEI (UAM-CSIC), C/ Faraday 7, 28049, Madrid, Spain

ARTICLE INFO

Keywords:

Oxidative stability
Rancimat test
Differential scanning calorimetry
Enzymatic glycerolysis
Microalgae oil
Rosemary extract

ABSTRACT

The oxidative stability of microalgae oil (MO) and its enzymatic glycerolysis product (GP) have been determined by using the accelerated oxidation methods differential scanning calorimetry (DSC) and Rancimat at temperatures in the range 50–90 °C. Kinetic analyses of MO and GP provide Arrhenius activation energy and activation enthalpy and entropy, temperature coefficients, Q_{10} and oxidative stability index at 20 °C (OSI_{20}), based on secondary and tertiary oxidation products. Susceptibility of microalgae oil to oxidation has been compared to that of fish and vegetable oils, with OSI_{20} values of 647 h for MO and 381 h for GP. The t_{coeff} and Q_{10} values are very similar to those observed for fish and vegetable oils. Protective effect from oxidation of a supercritical rosemary extract (RE) for both MO and GP have been evaluated. In the presence of this antioxidant, up to twofold increase of OSI_{20} has been obtained for MO. Lower protection for GP was observed. Activity antioxidant Index (AAI), related to the mechanism of action of the antioxidant, should be carefully examined for a reliable determination of OSI_{20} values.

1. Introduction

Polyunsaturated fatty acids (PUFAs) of long-chain eicosapentaenoic acid (EPA; 20:5, n-3) and docosahexaenoic acid (DHA; 22:6, n-3) show a range of health benefits with an appropriate intake in the diet. Food and Drugs Administration (FDA) and WHO/FAO recommends daily consumption of EPA and/or DHA from 140 to 600 mg to prevent cardiovascular conditions and they are recognized as safe with doses of up to 3 g/day (Marsol-Vall et al., 2020; Yang & Chiang, 2017). The benefits of EPA and DHA include suppression of vascular inflammation with strong cardioprotective effects. DHA shows benefits in the visual and cognitive functions of new-borns babies and children due to, its role as a component of synaptic membrane in brain and retina. Related with this, several studies have shown neuroprotective effect against neurodegenerative diseases, such as Parkinson, anti-aging function, protective suppression in colon cancer cells and reduction of developing diabetes illness (Lv et al., 2015; Yang & Chiang, 2017).

The consumption of oils rich in PUFAs (particularly EPA and DHA) in the form of supplements has gained recognition by consumers over the years due to the beneficial effects on health and the reduced risk of cardiovascular diseases. For decades, these oils have been obtained from fish sources, such as salmon and tuna. The increase in demand for these products by today's society, and factors such as overfishing and consequently negative impact on environment, have generated the need to look for new alternative sources to obtain them (Fedorova-Dahms et al., 2011; Lv et al., 2015; Marsol-Vall et al., 2020). In this way, large scale fermentation has permitted to by-pass marine food chain, producing EPA and DHA from microalgae species. *Schizochytrium* sp. microalgae oil (MO) contains up to 45% DHA and 10% EPA (w/w), which means a PUFA total percentage as high as 60–70%. MO is accepted as a safe product and available for dietary supplements and food use in general (Marsol-Vall et al., 2020).

Although MO has numerous benefits, it is also necessary to deal with some problems derived from its profile of fatty acids, which is abundant

Abbreviations: MO, microalgae oil; GP, glycerolysis product; RE, supercritical rosemary extract; EPA, eicosapentaenoic acid; DHA, docosahexaenoic acid; DSC, differential scanning calorimetry; OSI, oxidative stability index; AAI, activity antioxidant index.

* Corresponding author.

E-mail addresses: celia.banbares@uam.es (C. Bañares), assamae.chabni@uam.es (A. Chabni), guillermo.reglero@uam.es (G. Reglero), carlos.torres@uam.es (C.F. Torres).

<https://doi.org/10.1016/j.lwt.2022.114150>

Received 14 June 2022; Received in revised form 2 November 2022; Accepted 4 November 2022

Available online 11 November 2022

0023-6438/© 2022 The Authors. Published by Elsevier Ltd. This is an open access article under the CC BY-NC-ND license (<http://creativecommons.org/licenses/by-nc-nd/4.0/>).

in DHA. Regarding digestibility and bioaccessibility of MO, we must take into consideration different factors. PUFAs show low hydrolysis rate by the pancreatic lipase due to the curvature generated by the double bonds in their structure. Also, fatty acid residues longer than 18 carbon atoms exhibit lower degrees of hydrolysis in the presence of pancreatic lipase, and also, DHA located at the *sn*-1,3 position is not adequately hydrolyzed by pancreatic lipase. All these factors reduce the digestibility and absorption rate of ingested MO, and consequently, reduce the bioavailability of DHA (Na & Lee, 2020; Ye et al., 2018).

Enzymatic modification and particularly enzymatic glycerolysis of these oils arise as a great alternative to obtain mono-, di- and triacylglycerols in a mixture with better self-dispersion and emulsion properties. Likewise, glycerolysis products (GP) resemble intestinal digestion natural products and, thus, they are highly biocompatible and thus suitable as lipid delivery systems in formulations of functional foods and nutritional supplements of high bioavailability and bioefficiency. Additionally, these enzymatic processes are industrially scalable, environmentally clean and give rise to potentially self-emulsifying lipid mixtures that avoid addition of synthetic emulsifiers or other additives (Corzo-Martínez et al., 2016).

Another important matter to consider with MO is that oils with a large ratio of PUFAs are easily oxidized due to the presence of numerous double bonds in the hydrocarbonated structure. This fact reduces the nutritional value, produces undesirable odors, flavors, and colors, and affect negatively the quality of edible oils (Yin et al., 2021). Therefore, it is important to study the susceptibility to oxidation of this oil with the aim of improving the conditions of processing and storage. Accelerated techniques, such differential scanning calorimetry (DSC) and Rancimat test, are the key methods to assess the oxidative stability of oils (Bañares et al., 2019). Using these techniques, it is possible to obtain kinetic parameters which characterize the oxidation process of fats and oils and also estimate their shelf-lives, measured as the extrapolated oil stability index (OSI) at 20 °C in a representation of log(OSI) vs. temperature. It is particularly relevant to study the oxidative stability of oils according to the following criteria: i) two accelerated methods should be compared for consistency, ii) selecting a wide range of temperatures appropriate for the oil under study, iii) performing enough replicate assays at each temperature, and finally estimating the self-life as the extrapolated OSI value at 20 °C, i.e., OSI₂₀.

Although MO contains intrinsic antioxidants such phenolic compounds and carotenoids which may play protective effects against oxidation, the amounts present in the oil are usually not sufficient for prolonged protection (Yin et al., 2021). Therefore, the best strategy to improve the shelf life and oxidative stability of MO is by adding external antioxidants. In this sense, rosemary extract (RE) has been used extensively in food industry as a technological antioxidant. In addition, RE has shown various beneficial effects for health, such as anti-inflammatory, anticarcinogenic, antibacterial and antifungal. About 90% of the activity of RE as an antioxidant is associated with the compounds carnosic acid and carnosol. These compounds can neutralize hydroperoxide radicals. This has strong effects on lipid peroxidation during the oxidative process since it inhibits its propagation and consequently the yield of primary oxidation products. This effect has been shown to be higher in rosemary extract than in antioxidants, such butylated hydroxytoluene (BHT) and butylated hydroxyanisole (BHA) (Kaur et al., 2021).

The present work describes the oxidative stability of *Schizochytrium* sp.sp. microalgae oil and its glycerolysis product by the accelerated methods Rancimat and DSC in the temperature range 50–90 °C. Primary and secondary oxidation products have been evaluated as a function of time for both MO and GP. Kinetic analyses of the data has provided us with Arrhenius activation energy and pre-exponential factors, activation thermodynamic magnitudes (enthalpy and entropy), OSI at 20 °C (OSI₂₀) and temperature coefficients, and Q₁₀ values. To evaluate the antioxidant effect of a supercritical rosemary extract and to improve the oxidative stability of both MO and GP, the same accelerated methods

have been applied to samples including proper concentrations of this antioxidant. This work provides a robust methodology to study the oxidative stability of marine oils and their glycerolysis products, rich in DHA, and its possible stabilization with bioactive antioxidants such as supercritical rosemary extract.

2. Materials and methods

2.1. Chemicals and reagents

Microalgae oil (MO) sourced from the marine microalgae *Schizochytrium* sp.sp. was supplied by Progress Biotech (Capelle aan den IJssel, Netherlands) and stored under modified atmosphere of nitrogen at 4 °C. Glycerolysis product (GP) from microalgae oil was obtained following the methodology developed by Corzo et al. (2016) Corzo et al. (2016) with slight modifications. In brief, 10 g of MO were added to a 120 mL flask containing 1 g of glycerol (MO to glycerol molar ratio of 1:1). The mixture was thermostated at 40 °C with continuous agitation (200 rpm). Reaction was started with the addition of commercial lipase (*Candida antarctica*) in an enzyme to MO ratio of 1:10 (w/w) for 24 h hours. The product of reaction is recovered by filtering under vacuum (Corzo-Martínez et al., 2016). Rosemary antioxidant supercritical extract (RE) was obtained from Flavex Naturextrakte GmbH (Rehlingen-Siersburg, Germany) with a phenolic diterpenes content >10% (carnosic and carnosol acids). RE dosage in MO and GP were carried out in an amber vial under nitrogen stream, at 40 °C during 30 min at 900 mg/kg by magnetic stirring until a homogenous mixture is obtained for later use in the study.

Pure standards for chromatography analysis of microalgae oil monoacylglycerols (MAG) and diacylglycerols (DAG); were obtained by Solid Phase Extraction (SPE) from the GP using silica gel cartridge from Supelco-Merck Group (Darmstadt, Germany). The step-elution was carried out following the procedure reported by Ingalls et al. (Ingalls et al., 1993). Pure standard of FFA from microalgae oil was obtained by saponification process by Torres et al. (Torres et al., 2007). Isooctane was supplied by Carlo Erba Reagents (Val de Reuil, France). Methyl-tertbutyl ether (MTBE), hexane, chloroform and propan-2-ol were supplied by Lab-Scan (Gliwice, Poland). Formic acid (98% purity) was provided by Panreac (Barcelona, Spain). All solvents are of HPLC grade.

2.2. Analytical methods

2.2.1. Fatty acid profile of MO sample

MO was transformed into the corresponding fatty acid methyl esters (FAMES) by using the BF₃ derivatization method AOAC 996.06 (Rozema et al., 2008). For that purpose, an MO sample (50 mg) was dissolved in 1 mL hexane and then 1 mL of a 0.5 mol/L solution of sodium methoxide in methanol was added. The resulting solution was mixed using a vortex (Heidolph Reax top) and the mixture was incubated during 5 min at a temperature of 100 °C. 1 mL of a solution of BF₃-methanol 14% (w/w) was added and the mixture was mixed again in the vortex for 1 min, and later incubated by another 5 min at 100 °C. The next step consisted in adding 1 mL of hexane and 1 mL of NaCl (saturated aqueous solution) to the mixture. The resulting solution was then mixed again by approximately 2 min at 25 °C. The hexane phase was dehydrated using sodium sulphate, from where the FAMES were recovered. After 2 h, the FAMES solution was allocated in a previously weighted 8 mL vial. A FAMES residue was obtained in the vial by evaporating the solvent under nitrogen atmosphere.

A solution of the FAMES residue in hexane was prepared at a concentration of 15 mg/mL and a sample of 1 µL was injected into the gas chromatograph (Agilent 6850 N Network GC System) hosting a column HP-88 (length 30 m, internal diameter 0.25 mm). Temperature of injector was 220 °C and the flame ionization detector (FID) was maintained at 250 °C. The temperature ramp started at 50 °C and was increased at 15 °C min⁻¹ rate up to a maximum of 180 °C. A second

temperature ramp at a rate of $15\text{ }^{\circ}\text{C min}^{-1}$ followed until a final temperature of $220\text{ }^{\circ}\text{C}$ was reached, which was kept fixed during 10 min.

For quantification purposes, a calibration curve of ethyl oleate (utilized as external standard) was carried out. Agilent ChemStation Rev. 4B.03.01 software (Wilmington, DE, USA) was utilized for data acquisition and integration. All analyses were performed by duplicate and data are expressed as mean \pm standard deviation (SD).

2.2.2. Lipid profiles of MO and GP samples

GC analyses of MO sample were carried out using a gas chromatograph (Agilent 7820A, Santa Clara, USA) hosting on-column injection coupled to a FID detector. A HP-5MS capillary column, 5% phenyl methyl silicone (7 m length, 0.25 mm internal diameter, 0.25 μm thickness). A sample of 0.2 μL was injected. Injector temperature was $50\text{ }^{\circ}\text{C}$ and that of the detector was maintained at $340\text{ }^{\circ}\text{C}$. The temperature ramp started at $60\text{ }^{\circ}\text{C}$, with an increasing rate of $42\text{ }^{\circ}\text{C min}^{-1}$ up to $250\text{ }^{\circ}\text{C}$, which was kept constant by 20 min. Later on, temperature was increased up to $340\text{ }^{\circ}\text{C}$ at a rate of $25\text{ }^{\circ}\text{C min}^{-1}$, and then was kept fixed by another 35 min.

Lipid identification (FFA, TAG, DAG, MAG) was performed by determining the retention times (t_R), which were then compared to purified standards (see section 2.1). Once the lipids were identified, a quantitative analysis was performed by using the external standard method. The peaks in the chromatogram were analyzed by using the GC ChemStation software (Agilent, Boeblingen, Germany).

In the case of the GP samples, liquid chromatography with evaporative light scattering detection (LC-ELSD) was employed for lipid quantification by using an HPLC system (Agilent 1200 Series, Santa Clara, USA), hosting a (thermostated) column and quaternary pump, autosampler and vacuum degasser. The ELSD (Agilent 1260 Infinity) worked at $2 \times 10^5\text{ Pa}$ and $50\text{ }^{\circ}\text{C}$, with a gain of 4 (for accurate quantification of minor compounds). Separations were performed at $35\text{ }^{\circ}\text{C}$ in an Agilent Poroshell chromatographic column (Silica $2.7\text{ }\mu\text{m}$, $4.6 \times 100\text{ mm}$) using 2 mL min^{-1} flow rate and eluents isooctane 100%, 0.02% (v/v) formic acid in isooctane:MTBE (50:50, v/v) and MTBE:propan-2-ol (50:50, v/v), to obtain a ternary gradient system (Torres et al., 2005). A $1\text{ }\mu\text{L}$ injection volume was employed (about 20 μg of lipids). Data acquisition was carried out by using the Agilent ChemStation software (Agilent, Boeblingen, Germany).

2.2.3. Oxidation status

The evaluation of the initial oxidation status for both MO and GP was carried out by measuring the peroxide (PV) value and the p-anisidine (AnV) value, respectively, as primary and secondary oxidation indicators. These indicators were determined by colorimetric reactions performed in a commercial Oxitester (CDR FoodLabFat, Florence, Italy) by measuring the absorbance at 505 nm for PV and at 366 nm for AnV, according to the AOCS Official Method Cd 8-53 (PV). These determinations were performed by triplicate.

In addition, the total oxidative deterioration was evaluated by calculating the TOTOX quantity according to:

$$\text{TOTOX} = 2 \times \text{PV} + \text{AnV} \quad (1)$$

2.2.4. Rancimat and DSC methods

Oxidative stability for both MO and GP and antioxidant effects of RE on MO and GP were determined by using a Rancimat apparatus (743 Rancimat, Metrohm, Hesirau, Switzerland). MO samples of $3 \pm 0.01\text{ g}$ under a constant air flow (15 L h^{-1}) were used at the temperatures 50° , 60° , 70° , 80° and $90\text{ }^{\circ}\text{C}$. Oil stability indexes (OSIs) for MO and GP samples in the absence of the RE antioxidant and with the RE antioxidant present, were automatically registered as the proper endpoint, which was taken as the intersection point of the extrapolated curves (or plotted curves break point). OSI values were obtained in each treatment

as the average of three measurements. Antioxidant activity indexes (AAIs) were determined as (Nwosu et al., 1997):

$$\text{AAI} = \frac{\text{OSI}_w}{\text{OSI}_{wo}} \quad (2)$$

where OSI_w and OSI_{wo} correspond, respectively, to OSI values with antioxidant and without antioxidant present. Protective effect of the antioxidant correspond to $\text{AAI} > 1$, whereas $\text{AAI} = 1$ indicates no protective effect, and pro-oxidant effect is related to $\text{AAI} < 1$.

OSI values for GP and GP in the presence of RE antioxidant were determined by using DSC (Q100, TA instrument). Samples of 20 μL , which correspond to about 17 mg, were allocated in the chamber using an aluminum capsule and a nitrogen flow of 50 mL min^{-1} was first used. Temperature ramp at a rate of $10\text{ }^{\circ}\text{C/min}$ was used up to a fixed temperature. Once these conditions were set, nitrogen was replaced by air at 60 mL min^{-1} flow. Temperatures 50° , 60° , 70° , 80° and $90\text{ }^{\circ}\text{C}$ were evaluated. TA Universal Analysis 2000 software was used for the analysis of the results. The output was calculated as the amount of energy per gram per sample. The largest oxidation time (s_{max}) corresponds to the largest rate of oxidation (largest heat flow rate) with an accuracy of 0.005.

2.3. Kinetic data analysis

Linear regression of the Arrhenius equation,

$$\ln k = \ln A - \frac{E_a}{RT} \quad (3)$$

was employed for determining activation energies (E_a , kJ/mol) and pre-exponential factors (A , h^{-1}) from the slope and the intercept, respectively. The k represents the reaction rate constant, which in the present case corresponds to the reciprocal OSI (h^{-1}), i.e., $k = 1/\text{OSI}$. R is the molar gas constant.

The activation thermodynamic magnitudes are obtained using the equation (Steinfeld et al., 1999).

$$\ln\left(\frac{1}{\text{OSI}}\right) = \ln\left(\frac{k_B}{h}\right) + \frac{\Delta S^\ddagger}{R} - \frac{\Delta H^\ddagger}{R} \frac{1}{T} \quad (4)$$

where ΔS^\ddagger and ΔH^\ddagger are the activation entropy and enthalpy, respectively, and they are obtained from the linear regression $\ln(1/\text{OSI} \cdot 1/T)$ vs. $1/T$ from the slope and the intercept. In Eq. (4), h is the Planck constant, k_B is the Boltzmann constants and R is the molar gas constant.

Temperature coefficients (t_{coeff} , $^{\circ}\text{C}$) are obtained from the linear regression $\log(\text{OSI})$ vs. temperature (t , $^{\circ}\text{C}$) following the equation:

$$\log \text{OSI} = B + At \quad (5)$$

where the slope (A) corresponds to t_{coeff} and B is the intercept.

The temperature acceleration factor Q_{10} , which is defined as the increment of oxidation rate each $10\text{ }^{\circ}\text{C}$, is obtained as $(\text{OSI}_t)/(\text{OSI}_{t-10}^0)$.

2.4. Statistics

All determinations were performed in triplicate. The data were analyzed in terms of the variance (ANOVA). The ANOVA and regression analyses were performed according to the MStatC and SlideWrite softwares. Duncan's multiple range test was employed to determine significant differences between the means. P values < 0.05 were considered statistically significant.

3. Results and discussion

3.1. Profiles of lipids and fatty acids for MO and GP

The fatty acid profile of MO samples is listed in Table 1. The highest

Table 1
Fatty acid composition of MO.

Fatty acid (g/100g)	MO
Palmitic acid (C16:0)	17.61 ± 1.85
Palmitoleic acid (C16:1)	0.43 ± 0.04
Stearic acid (C18:0)	1.71 ± 0.10
Oleic acid (C18:1)	9.36 ± 1.09
Linoleic acid (C18:2)	1.33 ± 0.21
γ-Linolenic acid (C18:3)	0.33 ± 0.04
α-Linolenic acid (C18:3)	0.22 ± 0.02
Eicosapentaenoic acid (20:5)	0.74 ± 0.04
Behenic acid (C22:0)	1.46 ± 0.15
Docosapentaenoic acid (C22:5)	10.02 ± 0.33
Docosahexaenoic acid (C22:6)	54.86 ± 0.51
Others	1.93 ± 0.15
Total saturated FA	20.78 ± 1.98
Total monounsaturated FA	9.79 ± 1.02
Total polyunsaturated FA	67.51 ± 0.97

concentrations correspond to docosahexaenoic acid (DHA) (55%), and palmitic acid (18%), docosapentaenoic acid (EPA) (10%) and oleic acid (9%). The lowest values found are for eicosapentaenoic acid (0.74%), palmitoleic acid (0.43%), α-linolenic acid (0.22%) and γ-linolenic acid (0.33%). Overall, the proportion of SFA:MUFA:PUFA in the MO samples is 20:10:70. These results agree well with the ones published by Li et al. and Na et al. (Na & Lee, 2020; Yang & Chiang, 2017). In all cases found in the literature for microalgae oil, regardless of species, the highest proportion is always for DHA (ranging 23–55%) followed by palmitic acid (ranging 18–38%) (Lv et al., 2015; Yang & Chiang, 2017; Yin et al., 2021).

The lipid profiles of the MO and GP samples are shown in Table 2. Whereas TAG is the dominant acylglycerol in MO, substantial amounts of tri-, di- and monoacylglycerols are present in the GP due to the enzymatic glycerolysis process, being the DAG the predominant acylglycerol (50.2%). Wang et al. reported similar results where the most abundant acylglycerol after the glycerolysis process of *Schizochytrium* sp. oil was DAG (48.4%) (Wang et al., 2018).

Regarding the initial oxidative status of each product (results shown in Table 2), the peroxide values (PV) are 6.58 ± 0.16 and 7.8 ± 0.86 meq O₂/kg oil for MO and GP respectively, and the *p*-anisidine values (AnV) are 2.30 ± 0.28 and 3.75 ± 0.21 , for MO and GP, respectively. TOTOX values were 15.42 ± 0.60 for MO and 18.16 ± 1.93 for GP. According to the Global Organization for EPA and DHA (GOED), the limits for PV, AnV and TOTOX in DHA rich oils are 5 meq O₂/kg, 20 and 26, respectively (De Boer et al., 2018). Comparing these data with those obtained in this study, we conclude that the PVs of our products are slightly above the established limits but, nevertheless, the *p*-anisidine and TOTOX values fall within the accepted limits. Therefore, both MO and GP have good initial oxidative status and could be suitable for human consumption.

Making a comparison of the initial oxidative status from other studies of MO, PVs of 3.2 ± 0.5 meq O₂/kg for *Schizochytrium Aggregatum* microalgae oil (Lv et al., 2015) and 6 meq O₂/kg for the *Nannochloropsis*

species were reported (Gheysen et al., 2019). Regarding glycerolysis product, in the study of Corzo et al. an enzymatic glycerolysis of chimera shark liver oil was carried out (Corzo-Martínez et al., 2016). The final oxidation values were 16.56 ± 1.52 meq O₂/kg for peroxides and 4.53 ± 0.23 for *p*-anisidine (Corzo-Martínez et al., 2016). The values reported are larger than the present ones, and this could be due to the fact that the starting materials are different from those used here.

3.2. Oxidative stability for MO and GP by the DSC and Rancimat techniques

OSI values measured for MO by using Rancimat in the temperature range 50–90 °C with samples of 3 g and air flow of 15 L h⁻¹ are listed in Table 3. The error bars are calculated as the standard deviation of three experiments. As usual, OSI decreases with increasing temperature. Interestingly, the present OSIs measured by Rancimat for MO in the range of temperatures 70–90 °C are quite similar to the values reported by Yang et al. using the same methodology (Yang & Chiang, 2017).

Table 3 also includes the OSI values measured for GP using both DCS and Rancimat. The DSC test was applied using the same temperatures and the samples and air flow were of 17 mg and 60 mL min⁻¹, respectively. The OSIs determined for GP using Rancimat are in general larger than those measured by the DSC test at the same temperatures. At the same time, both OSI values for GP are smaller than the OSIs measured for MO by Rancimat. As expected, the OSI values for GP decrease monotonically as temperature increases.

The observed differences in OSI values for GP between both techniques (Rancimat vs. DSC) can be attributed to several factors. In the present study, we have found that the physic state of the sample is an important factor to consider when comparing the Rancimat and DSC tests. GP is semisolid at room temperature and its handling is more complex than for a liquid. Moreover, due to its melting point, it is required a transition of state from solid to liquid before the test itself. This could be relevant on the global oxidation process. In Rancimat, sample melting takes longer, whereas in DSC the melting is much faster due to the small amount used (17 mg for DSC as compared to 3 g for Rancimat). In addition, sample melting in DSC occurs under nitrogen flow. This difference has been mentioned before by Tan et al. (Tan et al., 2001) and Bañares et al. (Bañares et al., 2019). We conclude that the Rancimat test is more suitable for liquid samples than for semisolid fats. Furthermore, in the DSC test there is a difference between the heating flow in the sample capsule and that in another capsule employed as reference. Thus, the fast accumulation of peroxides correlates with the largest oxidation times. However, the Rancimat test deals with oxidation occurring at later stages, i.e. with the appearance of secondary volatile oxidation products.

The Arrhenius kinetics of OSIs measured for MO by Rancimat are shown in Fig. 1a. Fig. 1b depicts the kinetic data based on log (OSI) vs. temperature (in °C). Fig. 2a and b shows the kinetics of OSI for the GP samples using the DSC method. The linear regressions depicted in Figs. 1 and 2 indicate correlations with experimental values close to 99%. Considering the good fits obtained, this methodology can be considered as a good approach to obtain OSIs at other temperatures, as for instance, extrapolation to 20 °C to obtain OSI₂₀ values (see Tables 4 and 5). OSI₂₀ value for MO is 647 ± 119 h and for GP are 357 ± 43 h (DSC test) and 381 ± 70 h (Rancimat test).

As can be seen, in spite of the large uncertainty, OSI₂₀ is reduced by about 40–45% for GP in comparison with MO, which reflects a larger susceptibility of the enzymatic glycerolysis product to oxidation. The processing conditions, time, and temperature, and modifications in structure and composition of oils during the process of glycerolysis, can account for the lower oxidative stability. Recently, it has been proposed that by increasing or decreasing the exposure time to oxygen of unsaturated fatty acids, modifications in the position of the fatty acids in the structure of the lipids are produced, which affect stability (Kahveci et al., 2013). Other authors have found a negative impact of DAG and MAG on

Table 2
Lipid composition and initial oxidative status of MO and GP.

Lipids (g/100g)	MO	GP
Triacylglycerols	98.88 ± 0.21 ^a	26.10 ± 0.34 ^b
Diacylglycerols	0.73 ± 0.17 ^b	50.20 ± 0.20 ^a
Monoacylglycerols	0.38 ± 0.04 ^b	23.90 ± 1.20 ^a
Fatty acids	0.01 ± 0.003 ^a	–
Initial oxidative status		
PV (meq O ₂ /kg)	6.58 ± 0.16 ^a	7.8 ± 0.86 ^a
AnV	2.30 ± 0.28 ^a	3.75 ± 0.21 ^a
TOTOX	15.42 ± 0.60 ^a	18.16 ± 1.93 ^a

Significant differences in the same raw are indicated with different letters ($p < 0.05$).

Table 3

DSC and Rancimat test oxidative stability index (OSI) in the temperature range 50–90 °C for samples of MO and GP in absence and presence of RE antioxidant (200 and 7500 mg/kg). The antioxidant activity index (AAI) values of the different samples are included.

Temperature (°C)				Antioxidant presence RE					
	MO	GP		MO				GP	
	OSI (h) Rancimat	OSI (h) Rancimat	OSI (h) DSC	OSI (h) Rancimat 7500 mg/kg	OSI (h) Rancimat 200 mg/kg	AAI 7500 mg/kg	AAI 200 mg/kg	OSI (h) DSC 200 mg/kg	AAI 200 mg/kg
50	63.26 ± 1.35 ^a	49.59 ± 1.96 ^b	46.37 ± 3.27 ^b	101.03 ± 10.56 ^c	102.28 ± 0.84 ^c	1.59 ± 0.20	1.61 ± 0.05	71.23 ± 0.50 ^d	1.54 ± 0.12
60	36.78 ± 0.58 ^a	33.73 ± 1.63 ^{ad}	20.29 ± 0.25 ^b	52.25 ± 0.56 ^c	45.3 ± 3.24 ^{acd}	1.42 ± 0.04	1.23 ± 0.11	40.59 ± 0.21 ^d	1.99 ± 0.03
70	17.53 ± 0.81 ^{ad}	14.75 ± 0.55 ^{ab}	9.11 ± 0.73 ^b	43.03 ± 0.24 ^c	19.15 ± 0.04 ^d	2.45 ± 0.13	1.09 ± 0.05	19.00 ± 0.58 ^{ad}	2.08 ± 0.23
80	7.58 ± 0.02 ^a	7.80 ± 0.28 ^a	4.33 ± 1.24 ^a	23.14 ± 0.62 ^b	9.77 ± 0.21 ^c	3.05 ± 0.09	1.28 ± 0.02	12.20 ± 0.31 ^d	2.81 ± 0.88
90	3.79 ± 0.04 ^a	4.17 ± 0.08 ^{ab}	2.46 ± 0.13 ^b	10.09 ± 0.45 ^c	4.52 ± 0.07 ^d	2.66 ± 0.15	1.19 ± 0.03	6.56 ± 0.13 ^e	2.66 ± 0.19

Significant differences in the same raw are indicated with different letters ($p < 0.05$).

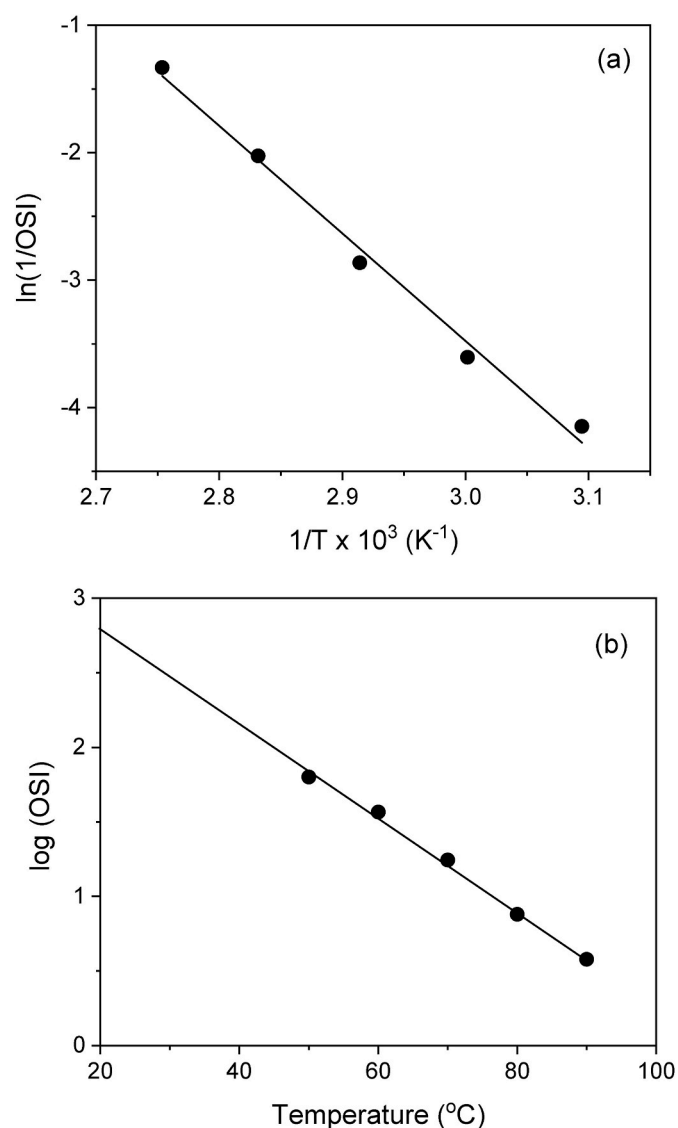


Fig. 1. (a) Arrhenius plot of OSI for MO at temperatures in the range 50–90 °C measured by the Rancimat test. (b) Plot of $\log(OSI)$ vs. temperature (°C) in the temperature range 50–90 °C for MO by the Rancimat test. Data are represented as mean values ($n = 3$).

the oxidative stability of edible oils due to their role as pro-oxidant molecules (Colakoglu, 2007; Miyashita & Takagi, 1986; Paradiso et al., 2014). The results obtained in the present work agree well with previous investigations, such as those by Wang et al. (Wang et al., 2019)

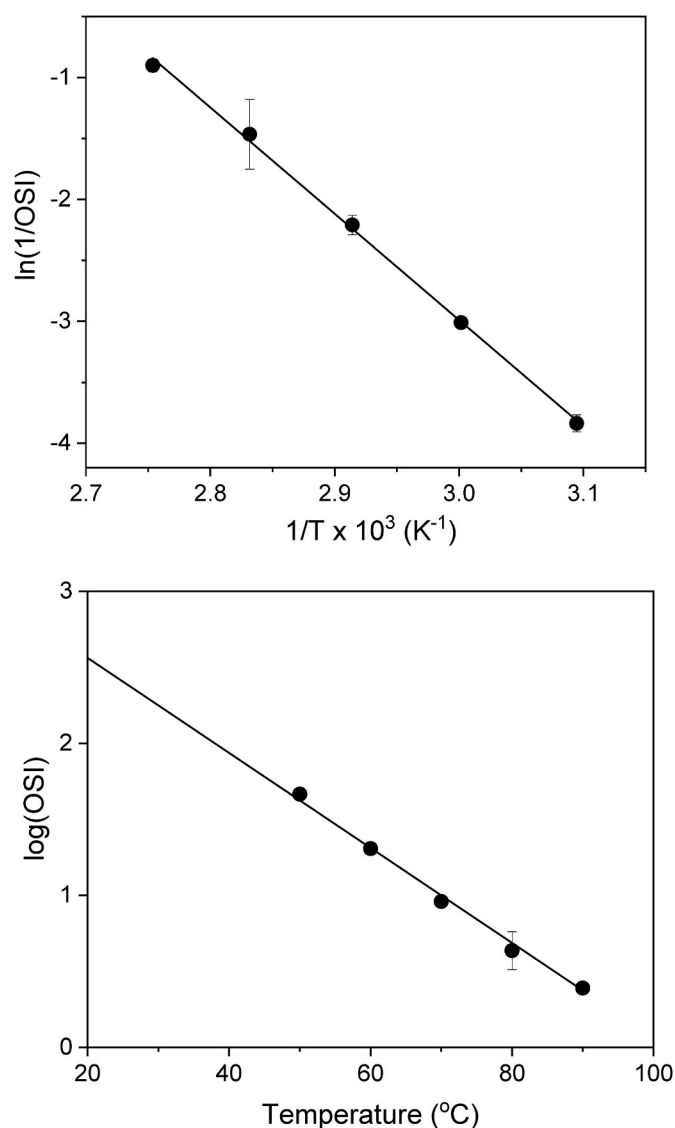


Fig. 2. (a) Arrhenius plot of the OSI values for GP at temperatures in the range 50–90 °C by the Rancimat test. (b) Plot of $\log(OSI)$ vs. temperature (°C) in the temperature range 50–90 °C for GP by the Rancimat test. Data are represented as mean values ($n = 3$).

and Kristensen et al. (Kristensen et al., 2005), where they attribute it to the fact that DAG is less thermally stable than TAG, due to the lower steric hindrance of DAG, which facilitates oxidative attack. All these reasons would support the lower oxidative stability of GP compared to

Table 4

Arrhenius parameters, A and E_a , activation enthalpy (ΔH^\ddagger), entropy (ΔS^\ddagger), temperature coefficient (t_{coeff}), Q_{10} and OSI_{20} obtained for MO, and MO in presence of RE at 200 and 7500 mg/kg, respectively, using Rancimat test in the temperature range of 50–90 °C.

Rancimat test							
Oil samples	$\ln(1/OSI) = a + b/T$		R^2	A (h^{-1})	E_a ($\text{kJ}\cdot\text{mol}^{-1}$)	ΔH^\ddagger ($\text{kJ}\cdot\text{mol}^{-1}$)	ΔS^\ddagger ($\text{J}\cdot\text{mol}^{-1}\cdot\text{K}^{-1}$)
	a	b					
MO	21.84 ± 1.35	-8440 ± 464	0.991	$3.05\cdot 10^9$	70.2 ± 3.9	67.3 ± 3.8	-92.4 ± 18.9
MO + RE (200 mg/kg)	23.59 ± 0.40	-9122 ± 139	0.999	$1.76\cdot 10^{10}$	75.8 ± 1.1	73.0 ± 1.1	-77.8 ± 3.3
MO + RE (7500 mg/kg)	14.93 ± 2.27	-6333 ± 779	0.956	$3.05\cdot 10^6$	52.7 ± 6.5	49.8 ± 6.4	-149.9 ± 11.2
Oil samples	$\log OSI = At + B$		R^2	Q_{10}	OSI_{20} (h)		
	$A = t_{\text{coeff}}$ ($^\circ\text{C}^{-1}$)	B					
MO	-0.032 ± 0.001	3.44 ± 0.08	0.996	2.03 ± 0.25	647 ± 119		
MO + RE (200 mg/kg)	-0.035 ± 0.001	3.73 ± 0.08	0.994	2.18 ± 0.17	1089 ± 201		
MO + RE (7500 mg/kg)	-0.023 ± 0.002	3.19 ± 0.18	0.965	1.83 ± 0.45	527 ± 218		

Table 5

Arrhenius parameters, A and E_a , activation enthalpy (ΔH^\ddagger), entropy (ΔS^\ddagger), temperature coefficient (t_{coeff}), Q_{10} and OSI_{20} obtained for GP, and GP in presence of RE at 200 mg/kg, using Rancimat and DSC test in the temperature range of 50–90 °C.

Rancimat test							
Oil samples	$\ln(1/OSI) = a + b/T$		R^2	$A \text{ (h}^{-1}\text{)}$	$E_a \text{ (kJ}\cdot\text{mol}^{-1}\text{)}$	$\Delta H^\ddagger \text{ (kJ}\cdot\text{mol}^{-1}\text{)}$	$\Delta S^\ddagger \text{ (J}\cdot\text{mol}^{-1}\cdot\text{K}^{-1}\text{)}$
	a	b					
GP	21.21 ± 0.64	$- 8219 \pm 229$	0.998	$1.6\cdot 10^9$	68.3 ± 1.9	66.7 ± 4.1	-94.2 ± 11.8
	$\log OSI = At + B$		R^2	Q_{10}	$OSI_{20} \text{ (h)}$		
	$A = t_{coeff} \text{ (}^\circ\text{C}^{-1}\text{)}$	B					
GP	$- 0.027 \pm 0.001$	3.11 ± 0.08	0.994	1.88 ± 0.33	381 ± 70		
DSC test							
Oil samples	$\ln(1/OSI) = a + b/T$		R^2	$A \text{ (h}^{-1}\text{)}$	$E_a \text{ (kJ}\cdot\text{mol}^{-1}\text{)}$	$\Delta H^\ddagger \text{ (kJ}\cdot\text{mol}^{-1}\text{)}$	$\Delta S^\ddagger \text{ (J}\cdot\text{mol}^{-1}\cdot\text{K}^{-1}\text{)}$
	a	b					
GP	23.16 ± 0.56	$- 8718 \pm 193$	0.998	$1.1\cdot 10^{10}$	74.1 ± 1.6	69.6 ± 1.6	-81.4 ± 4.7
GP + RE (200 mg/kg)	17.40 ± 0.75	$- 7010 \pm 259$	0.995	$3.6\cdot 10^7$	58.3 ± 2.1	55.4 ± 2.1	-129.3 ± 6.3
	$\log OSI = At + B$		R^2	Q_{10}	$OSI_{20} \text{ (h)}$		
	$A = t_{coeff} \text{ (}^\circ\text{C}^{-1}\text{)}$	B					
GP	$- 0.031 \pm 0.000$	3.17 ± 0.05	0.996	2.09 ± 0.23	357 ± 43		
GP + RE (200 mg/kg)	$- 0.025 \pm 0.000$	3.15 ± 0.04	0.996	1.82 ± 0.24	431 ± 40		

MO.

In any case, OSI_{20} is usually taken as a lower limit of the self-life. Extrapolation of the linear $\log(OSI)$ vs. t ($^\circ\text{C}$) trend is affected by numerous factors and should be considered with some caution. In particular, deviations from the linear trend can be expected at low temperatures, which makes extrapolation somewhat inaccurate (Bañares et al., 2019).

Temperature coefficients (t_{coeff}) and Q_{10} factors obtained from the $\log(OSI)$ vs. t ($^\circ\text{C}$) representation (Tables 4 and 5) are very similar for both MO and GP. The t_{coeff} value for MO is $(-3.2 \pm 0.1) \times 10^{-2} \text{ } ^\circ\text{C}^{-1}$ and those for GP are $(-2.7 \pm 0.1) \times 10^{-2} \text{ } ^\circ\text{C}^{-1}$ and $(-3.1 \pm 0.1) \times 10^{-2} \text{ } ^\circ\text{C}^{-1}$, depending on the test made (Rancimat vs. DSC). There is a good agreement between the present results and those obtained for vegetable oils (Hasenhuettl & Wan, 1992), which are in the range -2.78×10^{-2} to $-3.15 \times 10^{-2} \text{ } ^\circ\text{C}^{-1}$ (mean value $-3.01 \times 10^{-2} \text{ } ^\circ\text{C}^{-1}$), but significantly differ from those reported for fish oils (hake, anchovy, sardine), for which a mean value of $-7.5 \times 10^{-2} \text{ } ^\circ\text{C}^{-1}$ was reported by Méndez et al. (Méndez et al., 1996). In the study of Pazhouhanmehr et al., similar values are reported for kilka fish oil ($-3.02 \times 10^{-2} \text{ } ^\circ\text{C}^{-1}$) (Pazhouhanmehr et al., 2016). Variability of most of the data mentioned in literature could be explained by the oxidation pathways at different temperatures, metal ions reactivity, antioxidants and the reduction of the solubility of oxygen in oil by 25% for each 10 °C decrease (Robertson, 2007). Therefore, t_{coeff} is generally considered a representative magnitude of the oil under study (Zaanoun et al., 2014). The value of the Q_{10} factor is 2.03 ± 0.25 for oxidation of MO under Rancimat test, which indicates that a temperature increase of 10 °C, diminishes OSI by half. Similar Q_{10} values have been found for other oils, such as soybean oil ($Q_{10} = 2.05$), Echium oil ($Q_{10} = 2.04$), anchovy oil ($Q_{10} = 2.11$) and sardine oil ($Q_{10} = 2.14$)

(Bañares et al., 2019; Méndez et al., 1996). However, Pazhouhanmehr et al. reported lower Q_{10} values for kilka fish oil ($Q_{10} = 1.60$) (Pazhouhanmehr et al., 2016). The Q_{10} value obtained for GP is as the last value mentioned ($Q_{10} = 1.82\text{--}1.88$), which may reflect a larger susceptibility of GP to oxidation.

The Arrhenius parameters, A and E_a , and activation enthalpy and entropy, ΔH^\ddagger and ΔS^\ddagger , obtained by DCS and Rancimat are shown in Tables 4 and 5 for MO and GP, respectively. The activation energy E_a obtained for MO by the Rancimat test is $70.2 \pm 3.9 \text{ kJ mol}^{-1}$ and the corresponding activation magnitudes ΔH^\ddagger and ΔS^\ddagger are $67.3 \pm 3.8 \text{ kJ mol}^{-1}$ and $-92.4 \pm 18.9 \text{ J mol}^{-1} \text{ K}^{-1}$. Interestingly, the Arrhenius parameters found for GP are very similar, $68.3 \pm 1.9/74.1 \pm 1.6 \text{ kJ mol}^{-1}$ for E_a and $66.7 \pm 4.1/69.6 \pm 1.6 \text{ kJ mol}^{-1}$ and $-94.2 \pm 11.8/-81.4 \pm 4.7 \text{ J mol}^{-1} \text{ K}^{-1}$ for ΔH^\ddagger and ΔS^\ddagger , respectively. From this comparison, it is concluded that enzymatic glycerolysis process has a minor effect on the Arrhenius parameters of MO.

These values of activation energy E_a can be compared with those obtained for other vegetable oils at higher temperatures (100–140 °C) (Farhoosh, 2007; Tan et al., 2001). Activation energies reported for soybean and sunflower oils are 92.4 and 90.7 kJ mol^{-1} , respectively, at temperatures 100–130 °C, and for grape seed, corn and coconut oils are, respectively 99.9 , 88.1 , and 86.9 kJ mol^{-1} , in the temperature range 110–140 °C. Activation energy E_a clearly depends on the oil's PUFAs content. As it has been shown before, E_a increases for oils with a high content of monounsaturated and saturated fatty acids and it is reduced when polyunsaturated content increases (Adhvaryu et al., 2000; Ciemińska-Zytkiewicz et al., 2014; Kodali, 2005). Oils of animal origin with 20% PUFAs, such as fish oils, show a E_a value of 76 kJ mol^{-1} in the temperature range 4–60 °C (Sullivan et al., 2011), which is similar to those obtained here for MO and GP.

Regarding activation thermodynamic magnitudes, ΔH^\ddagger and ΔS^\ddagger , Kowalski et al. reported 74.9 kJ mol^{-1} and $-70.2 \text{ J mol}^{-1} \text{ K}^{-1}$, 82 kJ mol^{-1} and $-52.7 \text{ J mol}^{-1} \text{ K}^{-1}$, 84 kJ mol^{-1} and $-42.8 \text{ J mol}^{-1} \text{ K}^{-1}$, respectively, for soybean, rapeseed and sunflower oils by Rancimat (Kowalski et al., 2004). The oxidative stability of vegetable oils was evaluated by DSC (Tan & Man, 2002) and it was shown that the activation thermodynamic magnitudes ΔH^\ddagger and ΔS^\ddagger were larger for oils with higher content of PUFAs than for oils with lower PUFAs' content. Farhoosh et al. (Farhoosh et al., 2008) reported ΔH^\ddagger and ΔS^\ddagger values of $89.20 \text{ kJ mol}^{-1}$ and $-104.35 \text{ J mol}^{-1} \text{ K}^{-1}$ for soybean oil and of $83.64 \text{ kJ mol}^{-1}$ and $-116.66 \text{ J mol}^{-1} \text{ K}^{-1}$ for olive oil, respectively. The values of ΔH^\ddagger obtained in this work for MO and GP are smaller by about 20 kJ mol^{-1} than most of the reported values for vegetable oils and ΔS^\ddagger are more negative by about $20 \text{ J mol}^{-1} \text{ K}^{-1}$. Positive ΔH^\ddagger corresponds to an endothermic process to surpass the reaction barrier and negative ΔS^\ddagger indicates that the transition state species are more ordered than those of the reagents.

Comparative oxidative stability of MO against GP is clearly evidenced from the primary oxidation products determined by the peroxide value (PV) as a function of time for MO and GP under Rancimat test at 50°C . As shown in Fig. 3a, PV values increase much slowly with time for MO in comparison with GP. To obtain PV values larger than $45 \text{ meq O}_2/\text{kg}$, the MO sample needs 50 h, but it decreases to 25 h for GP. The increase of PV values as a function of time at 50°C is correlated with the primary oxidation products, but it is not enough for the evaluation of the time course of the oxidation, because primary products are transformed into secondary products. Therefore, the observations regarding the PV values can be interpreted as different rates of formation and transformation of primary oxidation products (Gray et al., 2010). Fig. 3b

depicts *p*-anisidine (AnV) as a function of time for the MO and GP samples using the Rancimat test at 50°C , as an indication of secondary oxidation products. AnV increases up to 55 h, the longest time measured, and the growth is clearly faster for GP than for MO. The results observed for PV and AnV to evaluate primary and secondary oxidation products clearly indicate that GP is more susceptible to oxidation than MO.

3.3. Antioxidant activity of rosemary extract on MO and GP

Since the OSI_{20} values determined for GP are shorter by about 40–45% compared to MO, we have investigated the role of the supercritical antioxidant rosemary extract (RE) in protecting MO and GP to oxidation, and thus in the possible increase of OSI_{20} by the presence of the antioxidant. This antioxidant is accepted for food use and according to Regulation (EC) No 1333/2008 of the European Parliament and of the Council of 16 December 2008 on food additives an upper limit of 50 mg of carnosic acid and carnosol Kg^{-1} in marine oils is permitted as an additive. The concentration of carnosic and carnosol utilized in this study which is reached at 200 mg/kg of RE comply with the allowed range. In addition, Rancimat tests for MO in presence of RE were carried out using concentrations of RE in the range $0\text{--}35000 \text{ mg/kg}$ to investigate the effects of the antioxidant at large quantities.

As shown in Fig. 4, OSI increases by a factor of 3, from 3 h without antioxidant up to $\approx 9 \text{ h}$ at 7500 mg/kg . As can be seen at concentrations larger than 15000 mg/kg , the increase of OSI levels out, reaching an asymptotic value of $\approx 13 \text{ h}$, and the factor increases slightly to ≈ 4 at the largest concentration used (35000 mg/kg).

By using 200 mg/kg of the antioxidant, OSI increases moderately (see Table 3). At 90°C OSI increases from 3.79 h in the absence of antioxidant to around 4.52 h with antioxidant present, i.e., a factor of 1.2. Considering the limits for the concentration of RE allowed by EFSA regulations, we have chosen 200 mg/kg to carry out the oxidative stability study of MO and GP when RE is present using DCS and Rancimat. The cross point of the tangent to the curve depicted in Fig. 4 corresponds to a concentration of 7500 mg/kg of RE, that was also chosen to study the oxidative stability. At this concentration of RE, OSI value increases by a factor of about 3. Hence, we have investigated the increase of OSI_{20} at two concentrations of RE, 200 mg/kg and 7500 mg/kg , with respect to MO.

OSI values obtained for MO with Rancimat as a function of temperature in the range $50\text{--}90^\circ\text{C}$ when using concentrations of 200 mg/kg and 7500 mg/kg of RE are shown in Table 3. A similar tendency to the one obtained for MO without antioxidant is observed in the presence of

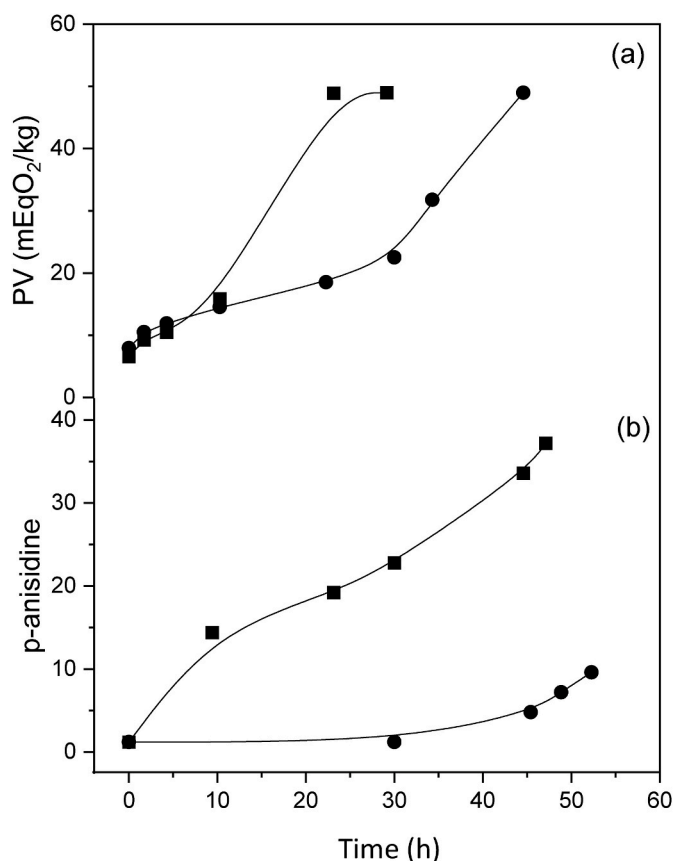


Fig. 3. (a) Peroxide value (PV) of MO (circles) and GP (squares) during application of Rancimat at 50°C as a function of time. (b) *p*-Anisidine of MO (circles) and GP (squares) during application of Rancimat at 50°C as a function of time. Data are represented as mean values ($n = 3$).

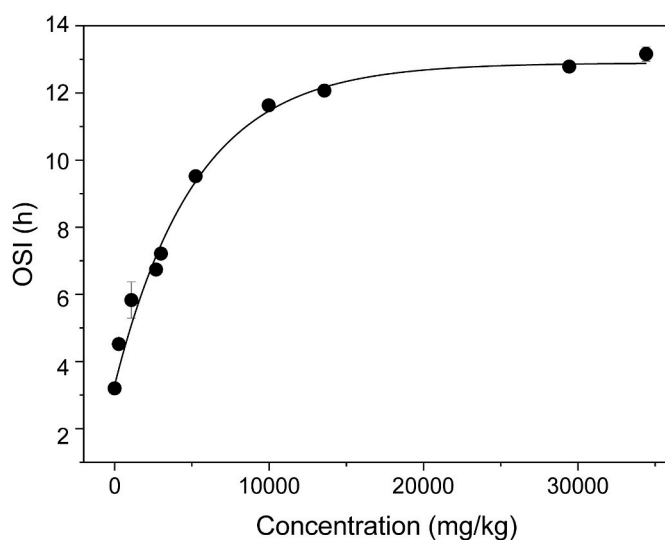


Fig. 4. RE dosage at different concentrations (mg/kg) in MO at 90°C by the Rancimat test. Data are represented as mean values ($n = 3$).

the antioxidant in a moderate concentration (200 mg/kg). Smaller values of OSI are obtained as temperature increases. Similar trend is also observed when using 7500 mg/kg of RE antioxidant, although OSI values are larger in the temperature range studied in comparison with 200 mg/kg. According to Rancimat, the oxidative protection of MO appears to be quite substantial at both antioxidant concentrations (about 60% OSI increment at the lower temperature of 50 °C). However, at the highest temperature (90 °C), the increase is more than 165% for 7500 mg/kg of RE and only 19% for 200 mg/kg of RE.

The antioxidant activity index (AAI) as a function of temperature for the RE antioxidant at the two concentrations (200 and 7500 mg/kg) used in the present work is depicted in Fig. 5. Values of AAI larger than 1 (Table 3) were obtained by using 200 mg/kg of RE in the temperature range studied in this work, being especially relevant the AAI value obtained from the extrapolations at 20 °C of about 1.7, which indicates a protective effect of RE on MO oxidation. Interestingly, the protection provided by RE at 200 mg/kg slightly decreases as temperature increases. This trend is also in agreement with the work of Bañares *et al.* for *Echium* oil, which showed that RE at doses of 200 mg/kg is a less effective at high temperatures (110 °C) than at middle temperatures (60 °C) (Bañares *et al.*, 2019). Other studies have shown a decrease of AAI for different antioxidants with increasing temperature, although it has been also pointed out that this behaviour is not an universal trend (Marinova & Yanishlieva, 1992, 2003; Réblová, 2012). On the contrary, by using RE at 7500 mg/kg, AAI increases with temperature and reaches values as high as 2.5–3 at the highest temperatures (80 and 90 °C). Similar trends have been found by Marinova *et al.*, where AAI (expressed as an effective factor index, *F*) for caffeic acid in sunflower oil was higher at 90 °C than at 22 °C (*F* = 12.9 and 6.5, respectively) (Marinova & Yanishlieva, 2003). The larger AAI values obtained as temperature increases could be explained by a change in the mechanism of action of the antioxidant during the oxidation process. However, when the AAI value is stable at various temperatures, it could indicate that the mechanism of antioxidant action is similar at the different temperatures. These data show that the oxidation stability results obtained at high temperatures can be used for a quantitative estimation at room temperature if no significant changes occur in the mechanism of antioxidant action at different temperatures (Marinova & Yanishlieva, 1992).

Arrhenius kinetic analyses and the log(OSI) vs. temperature representation were performed for MO with 200 mg/kg and 7500 mg/kg of RE under Rancimat, as depicted in the left and central panels of Fig. 6. As can be seen, the regressions presented in Fig. 6 show correlations with experimental values close to 99%. Arrhenius parameters, *A* and *E_a*,

activation enthalpy and entropy, ΔH^\ddagger and ΔS^\ddagger , the temperature coefficient t_{coeff} , along with Q_{10} and OSI₂₀ values are listed in Table 4. Temperature effect on the oxidation rate is determined by the activation energy *E_a*. Higher values of *E_a* indicate processes which are more dependent on temperature, whereas lower values of *E_a* correspond to processes without a clear tendency on temperature. Therefore, large *E_a* indicate that small temperature increments produce substantial changes in the oxidation rate. Values in between 40 and 400 kJ mol⁻¹ are representative of low and high *E_a* (Gregório *et al.*, 2018).

It can be concluded that there is a moderate dependency of the oxidation rate with temperature for MO and MO in presence of 200 mg/kg RE, since the values obtained are 70.2 ± 3.9 and 75.8 ± 1.1 kJ mol⁻¹, respectively. Surprisingly, the *E_a* obtained for MO in presence of 7500 mg/kg of RE is substantially smaller, i.e., 52.7 ± 6.5 kJ mol⁻¹, which seems to indicate that there is a low dependency of the oxidation rate with temperature for MO in presence of 7500 mg/kg RE antioxidant.

The pre-exponential factor (*A*) corresponds to the number of collisions that produce reaction, and thus a higher value of *A* indicates a larger probability of successful collisions that overcome the reaction barrier. In general terms, the *A* factor should be smaller when the antioxidant is present, which would indicate protective effects of the antioxidant employed. Indeed, the *A* factor for MO + 7500 mg/kg RE is lower by 3–4 decades in comparison with MO and MO + 200 mg/kg RE, which confirms the protective effect of the antioxidant at the high doses of 7500 mg/kg, especially at high temperatures.

Finally, protective effects of antioxidants can be evaluated at specific temperatures by the apparent rate constant $k = (1/\text{OSI})$. The smaller the rate *k*, the larger the antioxidant protection (Galvan *et al.*, 2013; Irigaray *et al.*, 2017). Here, *k* rates for MO at 90 °C are 0.26, 0.22 and 0.10 h⁻¹, without antioxidant, with antioxidant at 200 mg/kg of RE, and with antioxidant at 7500 mg/kg of RE, respectively, and at 50 °C these values were 0.016, 0.0098 and 0.0099 h⁻¹, respectively. These results confirm the protective effect of RE at the two doses employed on MO oxidation.

As shown in Table 4, OSI₂₀ values increase quite substantially (by 68% from 647 ± 119 h to 1089 ± 201 h) for MO and MO + RE 200 mg/kg, respectively. These values indicate that a concentration of 200 mg/kg of RE is a good dosage to increase the self-life of MO. In contrast, the OSI₂₀ value obtained for MO + RE 7500 mg/kg is 527 ± 218 h (a reduction of about 18%). This value, which is even lower than the OSI₂₀ of MO in the absence of antioxidant (647 ± 119 h), can be partially explained by the aforementioned arguments (see above), highlighting the risk of extrapolating to room temperature when the AAI values are not stable in the temperature range studied.

Next, the protection against oxidation of GP provided by the RE at 200 mg/kg by DSC test, was compared to the antioxidant protection obtained for MO in presence of RE at this concentration. Table 3 lists OSI values obtained for GP with and without antioxidant as a function of temperature in the range 50–90 °C. A similar trend to the one obtained for GP without antioxidant is observed when 200 mg/kg RE antioxidant is present, i.e., smaller OSI values are measured for higher temperature. The oxidative protection of GP is substantial with a 54% increment of OSI at the lower temperature studied (50 °C) and 167% increment at the highest temperature (90 °C).

The AAI values as a function of temperature for GP when using RE antioxidant at 200 mg/kg are always larger than 1 and increase from a moderate 1.21 at 20 °C to about 2.7–2.8 at the higher temperatures. This trend can be explained similarly to the case of MO+7500 mg/kg of RE. Probably the mechanism of action of RE changes significantly as temperature increases (Marinova & Yanishlieva, 1992).

Fig. 6 (right panels) shows the Arrhenius kinetic analyses and log(OSI) vs. temperature representation for GP with RE at 200 mg/kg present under the DSC technique. Again, linear trends are observed, and regression lines show correlation with experimental values close to 99%. It is remarkable that all kinetic parameters, *E_a*, *A*, t_{coeff} and Q_{10} , decrease quite clearly when the antioxidant RE at 200 mg/kg is present in

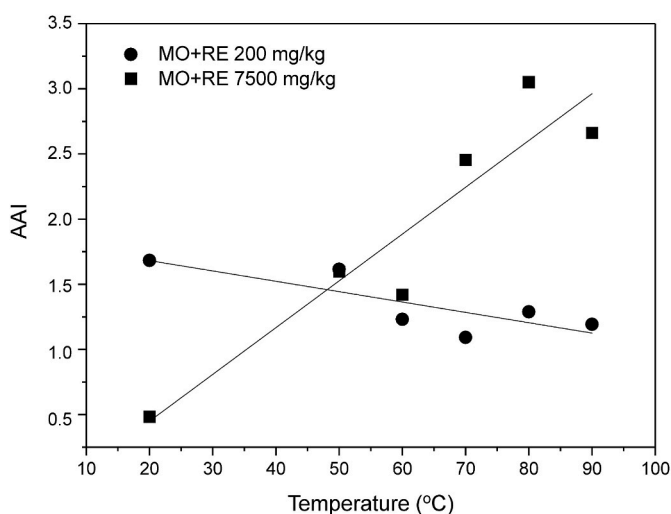


Fig. 5. AAI representation of MO + RE at 200 mg/kg (circles) and MO + RE at 7500 mg/kg (squares) in the temperature range 50–90 °C and the extrapolation at 20 °C.

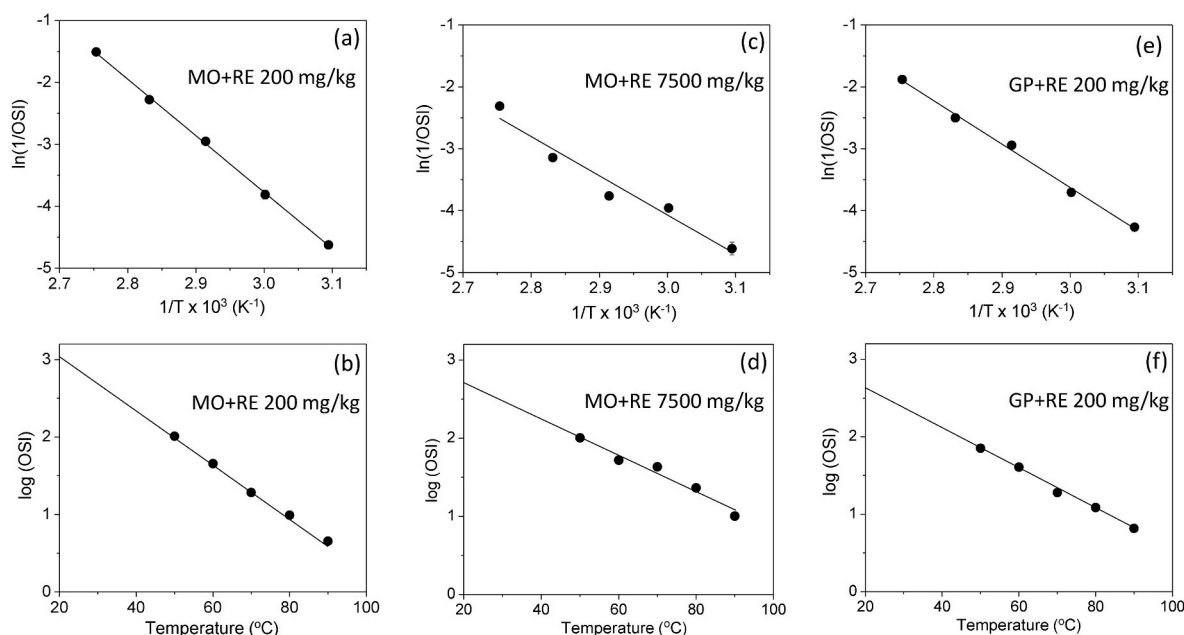


Fig. 6. (a) Arrhenius plot of OSI of MO + RE 200 mg/kg at temperatures in the range 50–90 $^{\circ}C$ by the Rancimat test. (b) Plot of $\log(OSI)$ vs. temperature ($^{\circ}C$) of MO + RE 200 mg/kg in the temperature range 50–90 $^{\circ}C$ by the Rancimat test. (c) Arrhenius plot of OSI of MO + RE 7500 mg/kg at temperatures in the range 50–90 $^{\circ}C$ by the Rancimat test. (d) Plot of $\log(OSI)$ vs. temperature ($^{\circ}C$) of MO + RE 7500 mg/kg in the temperature range 50–90 $^{\circ}C$ by the Rancimat test. (e) Arrhenius plot of the OSI values of GP + RE 200 mg/kg at temperatures in the range 50–90 $^{\circ}C$ by the DSC method. (f) Plot of $\log(OSI)$ vs. temperature ($^{\circ}C$) of GP + RE 200 mg/kg in the temperature range 50–90 $^{\circ}C$ by the DSC method.

comparison with GP without antioxidant (see Table 5), which indicates the less efficient protective effect of RE on the oxidation of GP in comparison with MO. As shown in Table 5, OSI_{20} values increase moderately for GP (by just 21% from 357 ± 43 h to 431 ± 40 h for GP and GP + RE 200 mg/kg, respectively) when using a 200 mg/kg RE antioxidant concentration, which confirms the less effective protective effect of RE for GP at this moderate concentration. These results can be explained by the different composition of GP, which is rich in DAG. DAGs are more susceptible to oxidation than TAGs in MO and therefore the OSI_{20} is affected by the different mechanism of action of RE at higher temperatures.

4. Conclusions

This work presents an extensive study of the oxidation stability of microalgae oil (MO) and its glycerolysis product (GP), carried out by using the accelerated techniques DSC and Rancimat test at temperatures in the range 50–90 $^{\circ}C$, determining secondary and tertiary oxidation products. The primary and secondary oxidation products are measured by the peroxide and *p*-anisidine values, respectively, obtained at different times in experiments carried out by Rancimat test at 50 $^{\circ}C$. Overall, the present results show that the glycerolysis product of microalgae oil is more susceptible to oxidation than microalgae oil and the latter is more susceptible to oxidation than other vegetable and fish oils.

Same tests have been carried out for microalgae oil and its glycerolysis product in the presence of rosemary extract (RE) as an antioxidant. A substantial protective effect has been observed for both microalgae oil and its glycerolysis product, although the protective effect is less efficient for the glycerolysis product. Extrapolations at room temperature to predict self-lives must be handled with caution, especially for the glycerolysis product, since its constituents are more susceptible to oxidation and the action mechanism of the antioxidant is subjected to stronger modifications as temperature increases. Experiments with other antioxidants would be very timely to evaluate better the protective effect of antioxidants on the enzymatic glycerolysis

product of microalgae oil.

CRediT authorship contribution statement

Celia Bañares: Investigation, Methodology, writing, Formal analysis, Data curation. **Assamae Chabni:** Investigation, Methodology, Formal analysis, Data curation. **Guillermo Reglero:** Funding acquisition, Project administration, Resources. **Carlos F. Torres:** Conceptualization, Methodology, Resources, writing.

Declaration of competing interest

The authors declare that they have no known competing financial interests or personal relationships that could have appeared to influence the work reported in this paper.

Data availability

Data will be made available on request.

Acknowledgements

This study has been funded by Ministerio de Ciencia e Innovación (project number PID 2020-119084RB-C21), Universidad Autónoma de Madrid (ALIBIRD, S2018/BAA-4343) and Fundación Ramón Areces (CIVP20A6607). Celia Bañares thanks Ministerio de Economía y Competitividad and the European Social Fund for a pre-doctoral FPI grant (BES-2017-080853). Assamae Chabni also thanks Comunidad de Madrid for a pre-doctoral grant (PEJD-2019-PRE/BIO-14522).

References

- Adhvaryu, A., Erhan, S. Z., Liu, Z. S., & Perez, J. M. (2000). Oxidation kinetic studies of oils derived from unmodified and genetically modified vegetables using pressurized differential scanning calorimetry and nuclear magnetic resonance spectroscopy. *Thermochimica Acta*, 364(1), 87–97.

- Bañares, C., Martin, D., Reglero, G., & Torres, C. F. (2019). Protective effect of hydroxytyrosol and rosemary extract in a comparative study of the oxidative stability of Echium oil. *Food Chemistry*, 290, 316–323.
- Ciemińska-Zytkiewicz, H., Ratusz, K., Bryś, J., Reder, M., & Koczoń, P. (2014). Determination of the oxidative stability of hazelnut oils by PDSC and Rancimat methods. *Journal of Thermal Analysis and Calorimetry*, 118(2), 875–881.
- Colakoglu, A. S. (2007). Oxidation kinetics of soybean oil in the presence of monoolein, stearic acid and iron. *Food Chemistry*, 101(2), 724–728.
- Corzo-Martínez, M., Vázquez, L., Arranz-Martínez, P., Menéndez, N., Reglero, G., & Torres, C. F. (2016). Production of a bioactive lipid-based delivery system from ratfish liver oil by enzymatic glycerolysis. *Food and Bioprocess Technology*, 100, 311–322.
- De Boer, A. A., Ismail, A., Marshall, K., Bannenberg, G., Yan, K. L., & Rowe, W. J. (2018). Examination of marine and vegetable oil oxidation data from a multi-year, third-party database. *Food Chemistry*, 254, 249–255.
- Farhoosh, R. (2007). The effect of operational parameters of the Rancimat method on the determination of the oxidative stability measures and shelf-life prediction of soybean oil [journal article]. *Journal of the American Oil Chemists' Society*, 84(3), 205–209.
- Farhoosh, R., Niazmand, R., Rezaei, M., & Sarabi, M. (2008). Kinetic parameter determination of vegetable oil oxidation under Rancimat test conditions. *European Journal of Lipid Science and Technology*, 110(6), 587–592.
- Fedorova-Dahms, I., Marone, P., Bailey-Hall, E., & Ryan, A. (2011). Safety evaluation of algal oil from *Schizochytrium* sp. *Food and Chemical Toxicology*, 49(1), 70–77.
- Galvan, D., Orives, J. R., Coppo, R. L., Silva, E. T., Angilelli, K. G., & Borsato, D. (2013). Determination of the kinetics and thermodynamics parameters of biodiesel oxidation reaction obtained from an optimized mixture of vegetable oil and animal fat. *Energy & Fuels*, 27(11), 6866–6871.
- Gheysen, L., Demets, R., Devaere, J., Bernaerts, T., Goos, P., Van Loey, A., De Cooman, L., & Foubert, I. (2019). Impact of microalgal species on the oxidative stability of n-3 LC-PUFA enriched tomato puree. *Algal Research*, 40, Article 101502.
- Gray, D. A., Payne, G., McClements, D. J., Decker, E. A., & Lad, M. (2010). Oxidative stability of *Echium plantagineum* seed oil bodies. *European Journal of Lipid Science and Technology*, 112(7), 741–749.
- Gregório, A. P. H., Romagnoli, E. S., Borsato, D., Galvan, D., & Spacino, K. R. (2018). Kinetic and thermodynamic parameters in biodiesel oxidation reaction in the presence of coffee leaves and sage extracts. *Sustainable Energy Technologies and Assessments*, 28, 60–64.
- Hasenhuettl, G. L., & Wan, P. J. (1992). Temperature effects on the determination of oxidative stability with the Metrohm Rancimat. *Journal of the American Oil Chemists' Society*, 69(6), 525–527.
- Ingalls, S. T., Kriaris, M. S., Xu, Y., DeWulf, D. W., Tserng, K.-Y., & Hoppel, C. L. (1993). Method for isolation of non-esterified fatty acids and several other classes of plasma lipids by column chromatography on silica gel. *Journal of Chromatography B: Biomedical Sciences and Applications*, 619(1), 9–19.
- Irigaray, B., Jachmanian, I., & Grompone, M. A. (2017). Antioxidant activity of a oryzanol concentrate by differential scanning calorimetry. *Journal of Food Research*, 7(1), 2017.
- Kahveci, D., Guo, Z., Cheong, L.-Z., Falkeborg, M., Panpipat, W., & Xu, X. (2013). Oxidative stability of enzymatically processed oils and fats. In L. Amy, N. Uwe, & P. Xiangqing (Eds.), *Lipid oxidation challenges in food systems* (pp. 211–242). AOCS Press.
- Kaur, R., Gupta, T. B., Bronlund, J., & Kaur, L. (2021). The potential of rosemary as a functional ingredient for meat products—a review. *Food Reviews International*. <https://doi.org/10.1080/87559129.2021.1950173>
- Kodali, D. R. (2005). Oxidative stability measurement of high-stability oils by pressure differential scanning calorimeter (PDSC). *Journal of Agricultural and Food Chemistry*, 53(20), 7649–7653.
- Kowalski, B., Ratusz, K., Kowalska, D., & Bekas, W. (2004). Determination of the oxidative stability of vegetable oils by differential scanning calorimetry and Rancimat measurements. *European Journal of Lipid Science and Technology*, 106(3), 165–169.
- Kristensen, J. B., Xu, X., & Mu, H. (2005). Diacylglycerol synthesis by enzymatic glycerolysis: Screening of commercially available lipases. *Journal of the American Oil Chemists' Society*, 82(5), 329–334.
- Lv, J., Yang, X., Ma, H., Hu, X., Wei, Y., Zhou, W., & Li, L. (2015). The oxidative stability of microalgae oil (*Schizochytrium aggregatum*) and its antioxidant activity after simulated gastrointestinal digestion: Relationship with constituents. *European Journal of Lipid Science and Technology*, 117(12), 1928–1939.
- Marinova, E. M., & Yanishlieva, N. V. (1992). Effect of temperature on the antioxidative action of inhibitors in lipid autoxidation. *Journal of the Science of Food and Agriculture*, 60(3), 313–318.
- Marinova, E. M., & Yanishlieva, N. V. (2003). Antioxidant activity and mechanism of action of some phenolic acids at ambient and high temperatures. *Food Chemistry*, 81(2), 189–197.
- Marsol-Vall, A., Aitta, E., Guo, Z., & Yang, B. (2020). Green technologies for production of oils rich in n-3 polyunsaturated fatty acids from aquatic sources. *Critical Reviews in Food Science and Nutrition*, 62(11), 2942–2962.
- Méndez, E., Sanhueza, J., Speisky, H., & Valenzuela, A. (1996). Validation of the Rancimat test for the assessment of the relative stability of fish oils. *Journal of the American Oil Chemists' Society*, 73(8), 1033–1037.
- Miyashita, K., & Takagi, T. (1986). Study on the oxidation rate and prooxidant activity of free fatty acids. *Journal of the American Oil Chemists' Society*, 63(10), 1380–1384.
- Na, B.-R., & Lee, J.-H. (2020). In vitro and in vivo digestibility of soybean, fish, and microalgal oils, and their influences on fatty acid distribution in tissue lipid of mice. *Molecules*, 25(22), 5357.
- Nwosu, C. V., Boyd, L. C., & Sheldon, B. (1997). Effect of fatty acid composition of phospholipids on their antioxidant properties and activity index. *Journal of the American Oil Chemists' Society*, 74(3), 293–297.
- Paradiso, V. M., Caponio, F., Bruno, G., Pasqualone, A., Summo, C., & Gomes, T. (2014). Complex role of monoacylglycerols in the oxidation of vegetable oils: Different behaviors of soybean monoacylglycerols in different oils. *Journal of Agricultural and Food Chemistry*, 62(44), 10776–10782.
- Pazhouhanmehr, S., Farhoosh, R., Sharif, A., & Kenari, R. E. (2016). Oxidation kinetics of common Kilka (*Clupeonella cultriventris caspia*) oil in presence of bene oils' unsaponifiable matter. *Food Chemistry*, 190, 748–754.
- Rěblová, Z. (2012). Effect of temperature on the antioxidant activity of phenolic acids. *Czech Journal of Food Sciences*, 30(2), 171–175.
- Robertson, G. L. (2007). Shelf life of packaged foods, its measurements and prediction. In A. L. Brody, & J. B. Lord (Eds.), *Developing new food products for a changing marketplace* (2nd ed., pp. 329–353). CRC Press.
- Rozema, B., Mitchell, B., Winters, D., Kohn, A., Sullivan, D., & Meinholz, E. (2008). Proposed modifications to AOAC 996.06, optimizing the determination of trans fatty acids: Presentation of data. *Journal of AOAC International*, 91(1), 92–97.
- Steinfeld, J. L., Francisco, J. S., & Hase, W. L. (1999). *Chemical kinetics and dynamics* (2nd ed.). Prentice Hall.
- Sullivan, J. C., Budge, S. M., & St-Onge, M. (2011). Modeling the primary oxidation in commercial fish oil preparations. *Lipids*, 46(1), 87–93.
- Tan, C., & Man, Y. C. (2002). Recent developments in differential scanning calorimetry for assessing oxidative deterioration of vegetable oils. *Trends in Food Science & Technology*, 13(9–10), 312–318.
- Tan, C., Man, Y. C., Selamat, J., & Yusoff, M. (2001). Application of Arrhenius kinetics to evaluate oxidative stability in vegetable oils by isothermal differential scanning calorimetry. *Journal of the American Oil Chemists' Society*, 78(11), 1133.
- Torres, C. F., Vázquez, L., Señoráns, F. J., & Reglero, G. (2005). Study of the analysis of alkoxyglycerols and other non-polar lipids by liquid chromatography coupled with evaporative light scattering detector. *Journal of Chromatography A*, 1078(1–2), 28–34.
- Torres, C. F., Vázquez, L., Señoráns, F. J., & Reglero, G. (2007). An efficient methodology for the preparation of alkoxyglycerols rich in conjugated linoleic acid and eicosapentaenoic acid. *Journal of the American Oil Chemists' Society*, 84(5), 443–448.
- Wang, X., Wang, X., Wang, W., Jin, Q., & Wang, X. (2018). Synthesis of docosapentaenoic acid-enriched diacylglycerols by enzymatic glycerolysis of *Schizochytrium* sp. oil. *Bioresource Technology*, 262, 278–283.
- Wang, Q., Xie, Y., Li, Y., Miao, J., & Wu, H. (2019). Oxidative stability of stripped soybean oil during accelerated oxidation: Impact of monoglyceride and triglyceride—Structured lipids using DHA as sn-2 Acyl-site donors. *Foods*, 8(9), 407.
- Yang, K.-M., & Chiang, P.-Y. (2017). Variation quality and kinetic parameter of commercial n-3 PUFA-rich oil during oxidation via Rancimat. *Marine Drugs*, 15(4), 97.
- Ye, Z., Cao, C., Liu, Y., Cao, P., & Li, Q. (2018). Triglyceride structure modulates gastrointestinal digestion fates of lipids: A comparative study between typical edible oils and triglycerides using fully designed in vitro digestion model. *Journal of Agricultural and Food Chemistry*, 66(24), 6227–6238.
- Yin, F., Sun, X., Zheng, W., Luo, X., Zhang, Y., Yin, L., Jia, Q., & Fu, Y. (2021). Screening of highly effective mixed natural antioxidants to improve the oxidative stability of microalgal DHA-rich oil. *RSC Advances*, 11(9), 4991–4999.
- Zaanoun, I., Gharby, S., & Bakass, I. (2014). Kinetic parameter determination of roasted and unroasted argan oil oxidation under Rancimat test conditions. *Grasas y Aceites*, 65(3), 33.